

FUNDAMENTAL STUDIES OF NEURAL STIMULATING ELECTRODES

**Fourth Quarterly Report
Covering Period May 29, 1995 to August 28, 1995
CONTRACT NO. N01-NS-4-2310**

**L. S. Robblee
S. F. Cogan
T. L. Rose
U. M. Twardoch
G. S. Jones
R. B. Jones**

**EIC Laboratories, Inc.
111 Downey Street
Norwood, Massachusetts 02062**

**Prepared for
National Institutes of Health
National Institute of Neurological
Disorders and Stroke
Bethesda, Maryland 20892**

September, 1995

This QPR is being sent to
you before it has been
reviewed by the staff of the
Neural Prosthesis Program

TABLE OF CONTENTS

| <u>Section</u> | <u>Page</u> |
|-----------------------------|-------------|
| 1 INTRODUCTION | 4 |
| 2 IF MICROELECTRODE STUDIES | 6 |
| 3 WORK FOR NEXT QUARTER | 24 |
| 4 REFERENCES | 24 |

LIST OF FIGURES

| | <u>Page</u> |
|---------|-----------------------------------------------------------------------------------------------------------------------------|
| Fig. 1 | Cyclic voltammograms acquired at Bak electrode 11A at a scan rate of 0.05 V/s at different times during a long term soak 10 |
| Fig. 2 | Cyclic voltammograms acquired at Bak electrode 11B at a scan rate of 200 V/s at different times during a long term soak 11 |
| Fig. 3 | Current function vs. $V^{1/2}$ for Bak electrode 11A from scan rate studies performed during long term soaking 12 |
| Fig. 4 | Current function vs. $V^{1/2}$ for Bak electrode 11B from scan rate studies performed during long term soaking 13 |
| Fig. 5 | Residual current vs. scan rate for Bak electrode 11A at different times during long term soaking 14 |
| Fig. 6 | Residual current vs. scan rate for Bak electrode 11B at different times during long term soaking 15 |
| Fig. 7 | Apparent capacitance vs. scan rate of Bak electrode 11A at different times during long term soaking 16 |
| Fig. 8 | Apparent capacitance vs. scan rate of Bak electrode 11B at different times during long term soaking 17 |
| Fig. 9 | Change in apparent capacitance measured at 0.05 V/s of Bak electrodes 11A and 11B 18 |
| Fig. 10 | Change in apparent capacitance measured at 200 V/s of Bak electrodes 11A and 11B 19 |
| Fig. 11 | Impedance at 1 kHz of Bak electrodes 11A and 11B at different times during long term soaking 22 |
| Fig. 12 | Bode plots of magnitude and phase angle of Bak electrodes 11A and 11B and different times during long term soaking 23 |

LIST OF TABLES

| | <u>Page</u> |
|---------|--------------------------------------------------------------------------|
| Table 1 | Cyclic voltammetric data for U-Mich CN8-49, site 1, scan rate study 1 21 |

1.0 INTRODUCTION AND SUMMARY

This report describes the work on NINDS Contract No. N01-NS-4-2310 during the period May 29, 1995 to August 28, 1995. As part of the Neural Prosthesis Program, the broad objectives of the present fundamental studies are: 1) to evaluate the electrochemical processes that occur at the electrode-electrolyte interface during pulsing regimens characteristic of neural prosthetic applications; 2) to establish charge injection limits of stimulation electrode materials which avoid irreversible electrochemical reactions; 3) to develop an *in vitro* method, which can be applied *in vivo*, for determining the electrochemical real area and stability of microelectrodes; 4) to develop new materials which can operate at high stimulation charge densities for microstimulation; and 5) to provide electrochemical and analytical support for other research activities in the Neural Prosthesis Program at NINDS.

The electrochemical studies of Ir microelectrodes which were initiated in the second quarter were concluded. Changes in electrochemical properties of a pair of Ir microelectrodes from Laboratory for Neural Control, NINDS, were followed for a total of 208 days soaking in PBS solution. Cyclic voltammetric studies utilizing Ru hexaamine to determine electrode dimensions based on a diffusion controlled process indicated that mass transport to these electrodes became altered after about 49 days of soaking for one electrode and 89 days for the other. The scan rate data suggested that there was a contribution to the faradaic current from a cavity produced by separation of the insulating film from the metal conductor. Apparent capacitance measurements also indicated an increase in electrochemically active surface area of both electrodes during the long term soak. The impedance at 1 kHz tended to decrease over the entire soaking period, but it fluctuated considerably so that it would be difficult to use that value alone to assess the electrode status. However, the impedance spectra demonstrated a change in both phase angle and magnitude after about 86 days of soaking. The general agreement between mass transport studies, apparent capacitance measurements and the change in impedance spectra provide evidence for a significant change in electrochemically active area, with the cyclic voltammetric data providing clearest evidence of the degradation of the seal at the insulator/metal interface after several weeks of soaking. These experiments have provided information in two areas. First, we have demonstrated that the electrochemical stability of this pair of Parvlenes

insulated microelectrodes is significantly greater than any previously tested electrodes of this type. Second, it appears that cyclic voltammetric measurements of apparent capacitance can be used to evaluate the electrochemical stability of metal microelectrodes. Further development of this protocol will be undertaken for adaptation to *in vivo* use.

2.0 Ir MICROELECTRODE STUDIES

Electrochemical studies of a dual hat-pin type of Ir microelectrode assembly were completed this quarter. This electrode assembly was submitted by the Laboratory of Neural Control (NINDS) as a test electrode for use in developing procedures for monitoring Ir microelectrode integrity and electrochemical surface area. Test procedures and results of the first 50 days of electrochemical testing were described in the Quarterly Progress Report No. 2. Since that report, the electrode assembly has been soaking in PBS solution and intermittent electrochemical testing using cyclic voltammetry and impedance spectroscopy was performed as described for a U-Mich probe in Quarterly Progress Report No. 3.

Cyclic Voltammetry Studies

An abbreviated cyclic voltammetry test protocol was employed to monitor electrode status during the soaking period from 50 days to 140 days. This protocol consisted of scan rate studies using only the scan rates 0.05, 10, 20, 50, 100 and 200 V/s. It was not practical to use the full range of sweep rates from 0.001 to 200 V/s as was done in earlier tests because of the continuing deterioration in the voltammetric response at slow scan rates due to electrolyte penetration beneath the insulator. Voltammetry was carried out in PBS and in solutions of Ru hexaammine in PBS. The testing in PBS included voltammetry in the old PBS solution in which the electrodes had been soaking since the prior solution change, and a second set of voltammograms in the new PBS immediately after a solution change. If Ru hexaammine studies were performed, then the PBS was deaerated. Thus we have obtained a history of the voltammetric responses of the microelectrodes in Ru hexaammine solution, in both old and new PBS, and in aerated and deaerated PBS for a soaking period up to 140 days.

Following the third scan rate study reported in Quarterly Progress Report No. 2, the electrodes remained soaking in PBS with periodic solution changes to minimize microbial growth. Two additional scan rate studies were performed after 89 days soaking and 140-141 days soaking to determine electrode dimensions based on diffusion controlled reduction of Ru hexaammine. However the voltammograms acquired in Ru hexaammine and in PBS had significant distortion, and the data could not be fit to any of the standard equations for calculating dimensions based on a diffusion controlled process. Some of these voltammograms are illustrated in Figures 1 and 2

where they are compared with voltammograms from the first three scan rate studies. The increase in the diagonal orientation of the curves coupled with the higher residual and charging current particularly at the slow scan rate indicate increasing electrolyte penetration between the insulator and the metal.

Figures 3 and 4 are plots of the current function $i(\nu)^{1/2}$ vs. $\nu^{1/2}$ for scan rates $> 1 \text{ V/s}$ for all the studies in which a background correction could be performed. The current is normalized to the Ru hexaamine concentration used in each experiment permitting a direct comparison of data acquired at different times. Referring to Figure 3 which contains data for electrode 11A, the plot of $i(\nu)^{1/2}$ vs. $\nu^{1/2}$ at 2 days is linear consistent with radial diffusion. In the plots for 26 days and 49 days $i(\nu)^{1/2}$ tends toward a constant value at scan rates above 2 V/s although there is some random fluctuation in the values. A constant value of $i(\nu)^{1/2}$ over a range of scan rates is characteristic of linear diffusion in that time domain. The transition from radial to linear diffusion behavior within the same range of scan rates between day 2 and day 26 suggests a change in electrode dimensions or exposed surface area. At 89 days, $i(\nu)^{1/2}$ shows a tendency toward increasing values at scan rates above 50 V/s , and this trend is even more pronounced in the plots for 135 days and 140 days. The increase in $i(\nu)^{1/2}$ at high scan rates is an indication of a thin layer volume contained within a cavity [Iwardoch, 1994], and is interpreted as evidence for further deterioration of the insulator-metal seal.

Figure 4 illustrates the data for electrode 11B. As for electrode 11A, the 2nd day plot of $i(\nu)^{1/2}$ vs. $\nu^{1/2}$ is nearly linear, and the 26 day plot is independent of scan rate. The plot obtained at 49 days shows a pronounced minimum in the $i(\nu)^{1/2}$ vs. $\nu^{1/2}$ curve, suggesting a more severe penetration of electrolyte beneath the insulator at that time than was observed for electrode 11A. Subsequent scan rate data for electrode 11B were not suitable for analysis because of additional deterioration of the voltammetric responses.

Although the later mass transport studies could not be used to determine electrode dimensions, nevertheless the shape of the $i(\nu)^{1/2}$ vs. $\nu^{1/2}$ plots provided qualitative evidence of the deterioration of the insulator-metal seal during the long soaking experiment with the possible growth of a thin layer volume of electrolyte beneath the insulator. While the method tells us about the quality of the insulator seal of this set of electrodes, nevertheless an additional goal of

these experiments is to develop a protocol which can be used with *in vivo* electrodes, and the Ru hexaammine protocol cannot be used for implanted electrodes. The protocol which might be adapted for *in vivo* use is a measurement of the background current in saline electrolyte at a potential where faradaic reactions are unlikely to contribute to the current. In this work, we have measured the background or residual current at 0 V vs. Ag/AgCl in cyclic voltammograms acquired in PBS. This quantity is assumed to be representative of capacitive charging without significant contribution from faradaic processes. Oxygen was investigated as a source of error in these measurements by acquiring voltammograms in aerated and deaerated PBS. These voltammograms indicated that oxygen had no effect on the magnitude of the current response at 0 V. The effect of an oxide film will eventually be examined in long term soaking studies of activated Ir. However, it is first necessary to evaluate the experimental approach using unactivated Ir electrodes.

Figure 5 contains plots of the residual current at 0 V vs. Ag/AgCl measured from cyclic voltammograms acquired in PBS at electrode 11A at various times during the electrode soaking period. Log scales are used on this graph, and on subsequent ones, solely to improve the separation of data points along both axes. There are relatively small differences in the residual current data obtained at 2, 26 and 49 days of soaking. This is consistent with the previously reported stability of electrode dimensions determined on the basis of the diffusion controlled process. After day 49 there is a general upward trend toward higher residual currents at all scan rates, with the greatest increase observed after day 131.

Residual current plots for electrode 11B are given in Figure 6. These plots also show a trend toward increasing residual current at all scan rates as a function of soaking time. However, for this electrode, a large increase in residual current was observed between days 5 and 23, as well as after day 13.

Figures 7 and 8 are plots of the apparent capacitance, C_{app} , of electrodes 11A and 11B. Apparent capacitance was calculated from the residual current, i.e., as follows

$$C_{app} = I_r / \text{scan rate}$$

If the residual current were due only to charging of the electrode double layer, then the capacitance would be constant for all scan rates, and an estimate of electrochemically active surface area (ESA) could be calculated by normalizing the capacitance to the capacitance of the Ir

metal = $25 \mu\text{F cm}^{-2}$. However, the more complex dependency of C_{app} on scan rate indicates that other processes in addition to double layer charging are contributing to the residual current. For the present study, we do not attempt to define what those processes might be because we are more interested in the relative change in residual current and C_{app} during soaking. Figures 9 and 10 show the relative change in C_{app} of both electrodes measured at a slow and fast scan rate, respectively. For both electrodes, C_{app} measured at 0.05 V s^{-1} (Figure 9) increased over the first 130 days by a factor of ~ 5 . Between 130 and 140 days, C_{app} of electrode 11A increased to ~ 25 times its initial value, and C_{app} of electrode 11B increased to ~ 15 times its initial value. A two-fold increase in C_{app} was measured from data acquired at 200 V s^{-1} (Figure 10) about two-fold over the 140 day period except for one measurement of a 4-fold increase for electrode 11B. The non-reproducibility of C_{app} regardless of the scan rate at which it was measured is an indication of an increase in exposed surface area. The difference between the 0.05 V s^{-1} and the 200 V s^{-1} results suggests that some of the exposed surface area is not accessible at the fast scan rate possibly because of iR drops beneath the insulator leading to non-uniform potential distribution at the faster scan rate. The results indicate that a cyclic voltammetric technique without an added depolarizer such as Ru hexaammine can be adapted for *in vivo* monitoring of microelectrode stability.

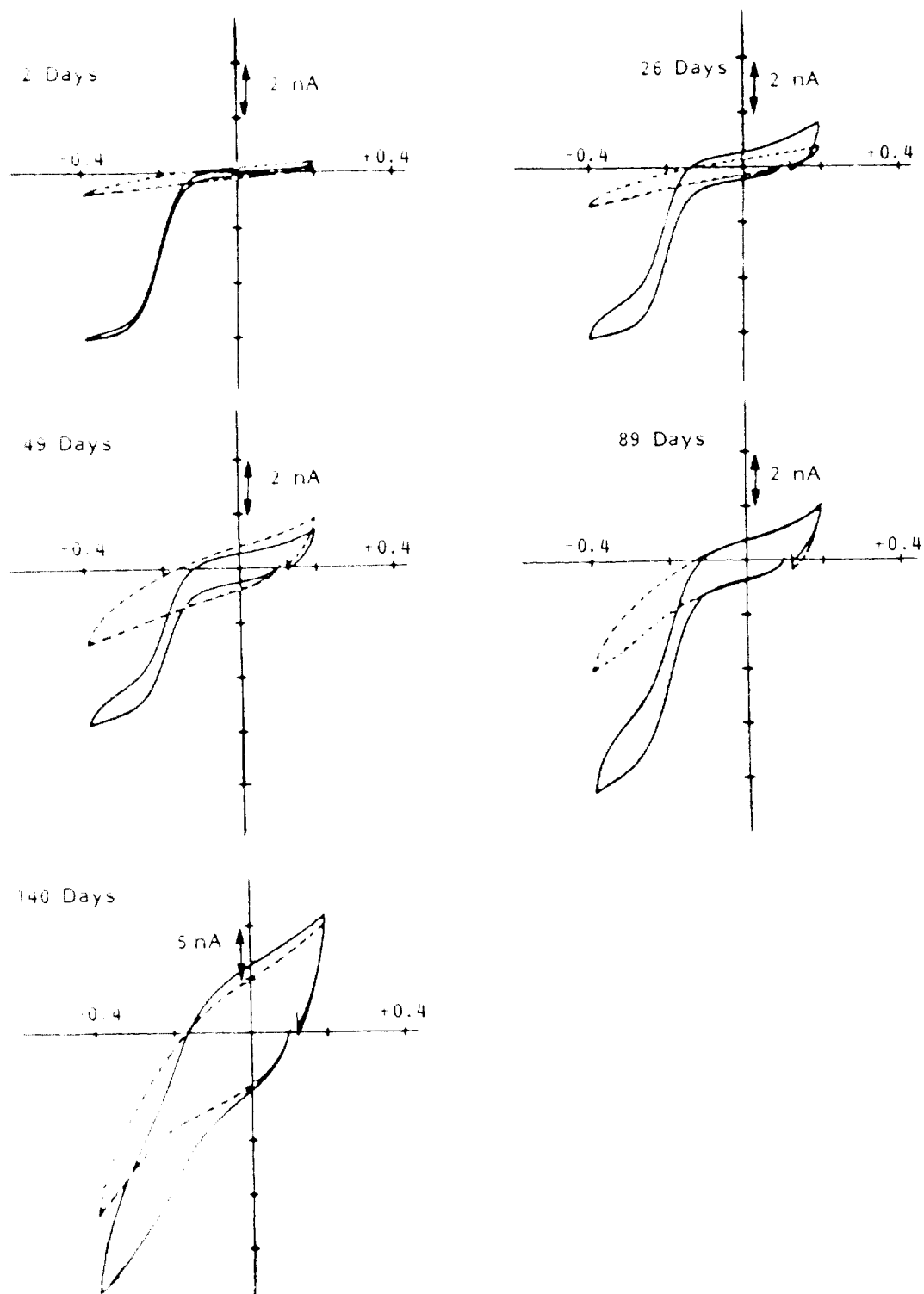


Figure 1: Cyclic voltammograms acquired at Bak electrode 11A at different times during long term soaking. Scan rate = 0.05 V/s. Solid line = in a solution of $[\text{Ru}(\text{NH}_3)_6]^{3+}$ in PBS. Broken line = in PBS. Potential is given as V vs. Ag/AgCl.

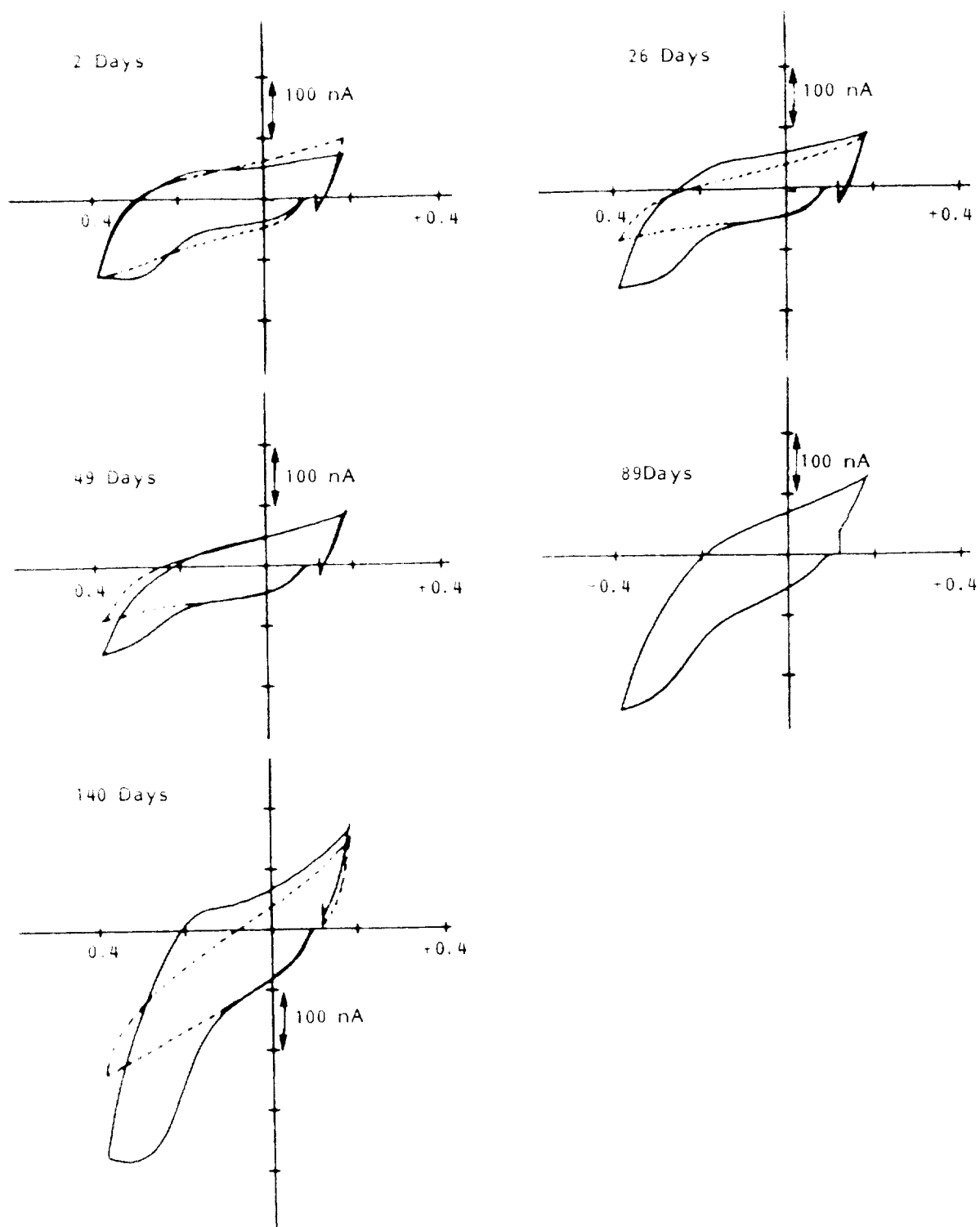


Figure 2. Cyclic voltammograms acquired at Bak electrode 11A at different times during long term soaking. Scan rate: 200 V/s. Solid line: in a solution of $[\text{Ru}(\text{NH}_3)_6]^{3+}$ in PBS. Broken line: in PBS. Potential is given as V vs. Ag/AgCl.

Iridium Microelectrode 11A Faradaic Response to Ru Hexaammine

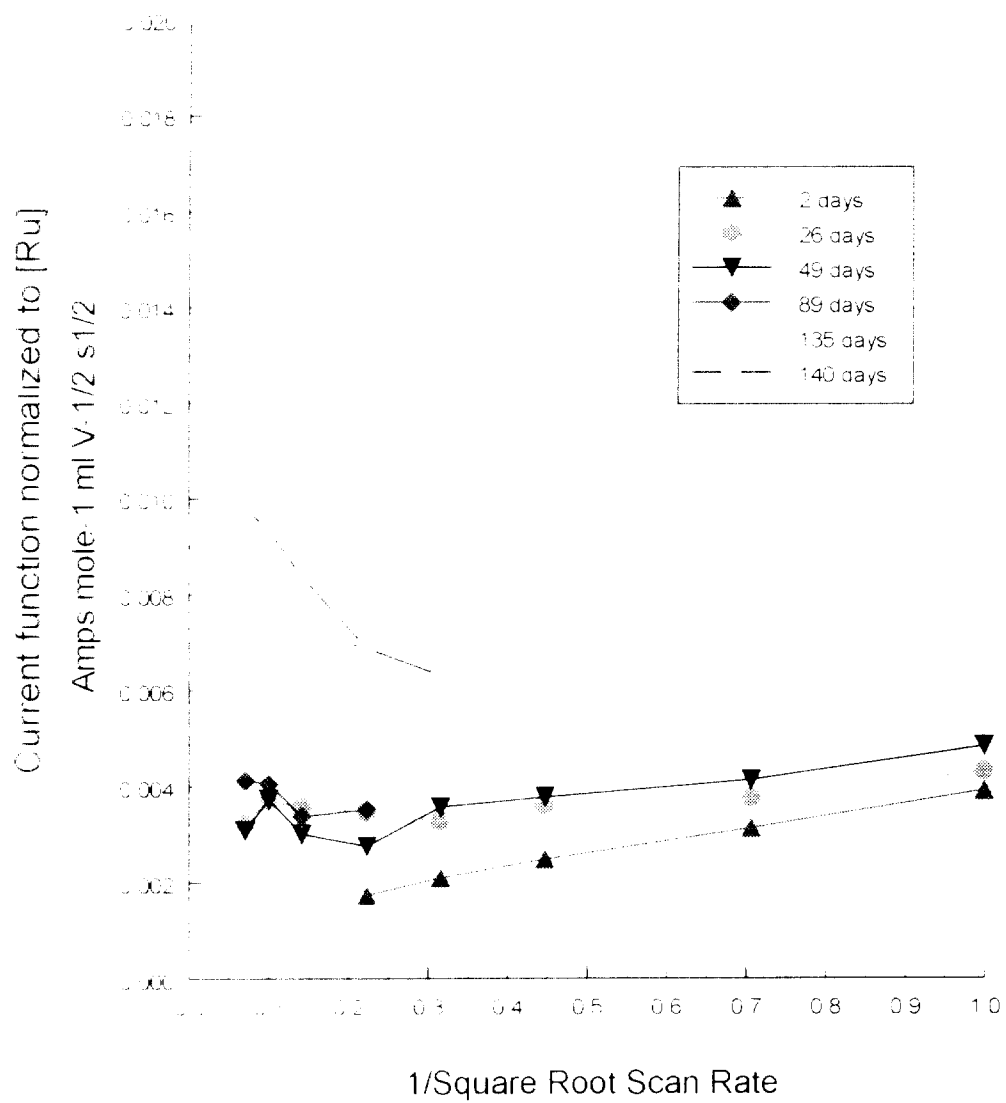


Figure 3 Current function vs $v^{-1/2}$ for Bak electrode 11A from scan rate studies performed during long term soaking

Iridium Microelectrode 11B Faradaic Response to Ru Hexaammine

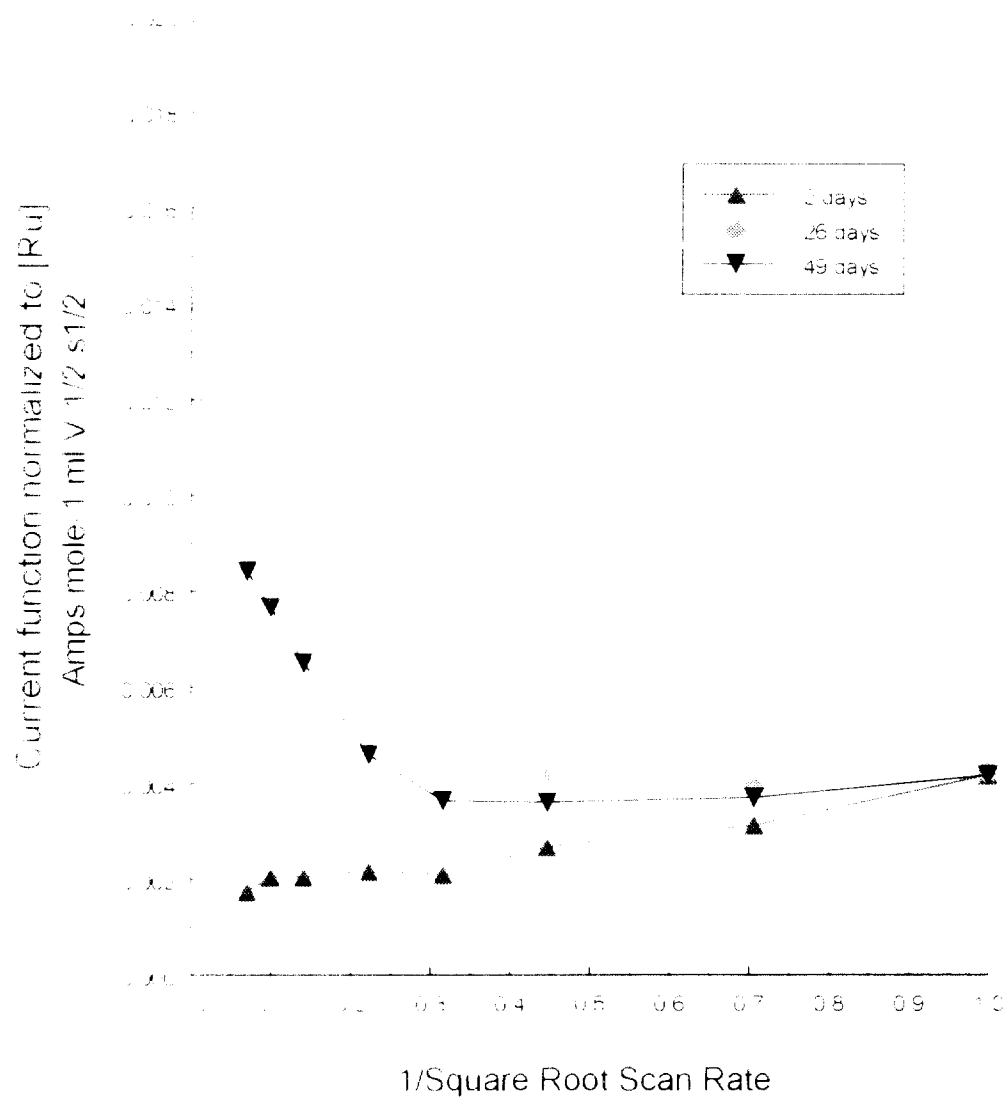


Figure 4 Current function vs. $V^{-1/2}$ for Bak electrode 11B from scan rate studies performed during long term soaking

Iridium Microelectrode 11A Residual current measured in PBS at 0 V vs Ag|AgCl

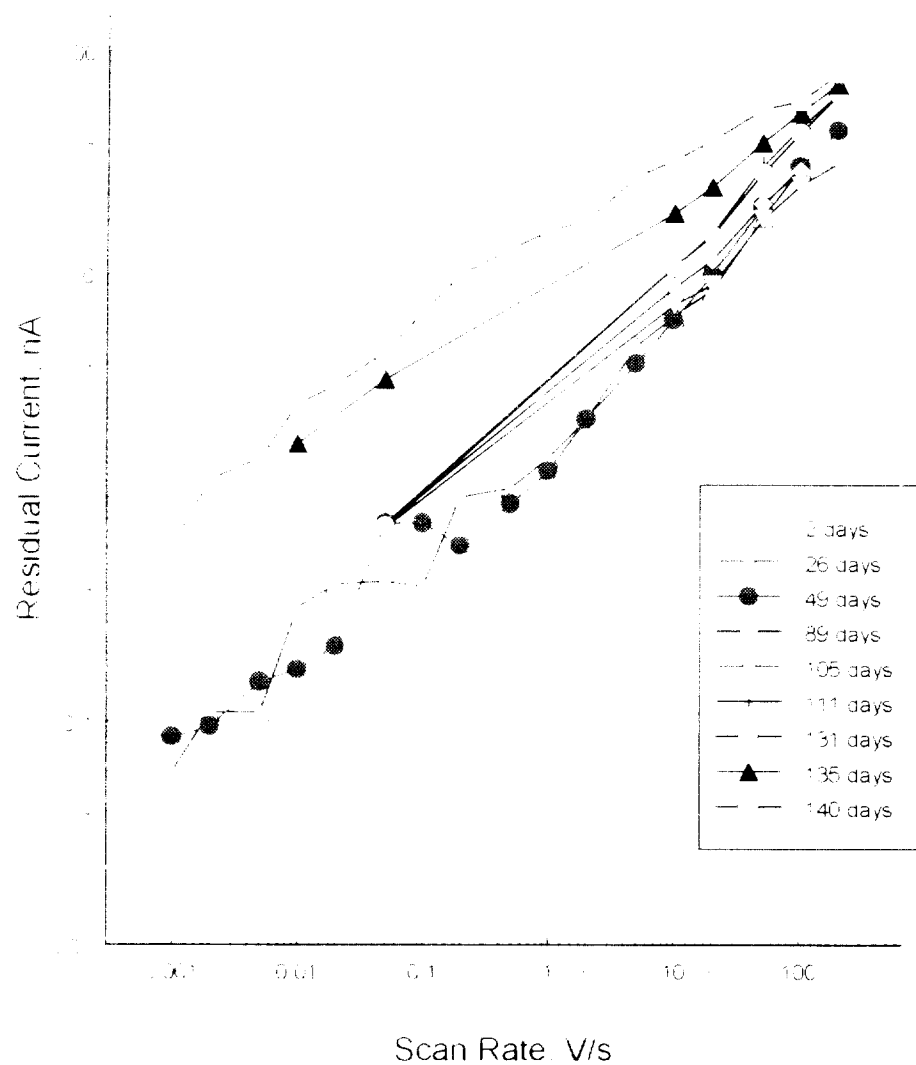


Figure 5 Residual current vs. scan rate for Bak electrode 11A at different times during long term soaking

Iridium Microelectrode 11B Residual current measured in PBS at 0 V vs Ag|AgCl

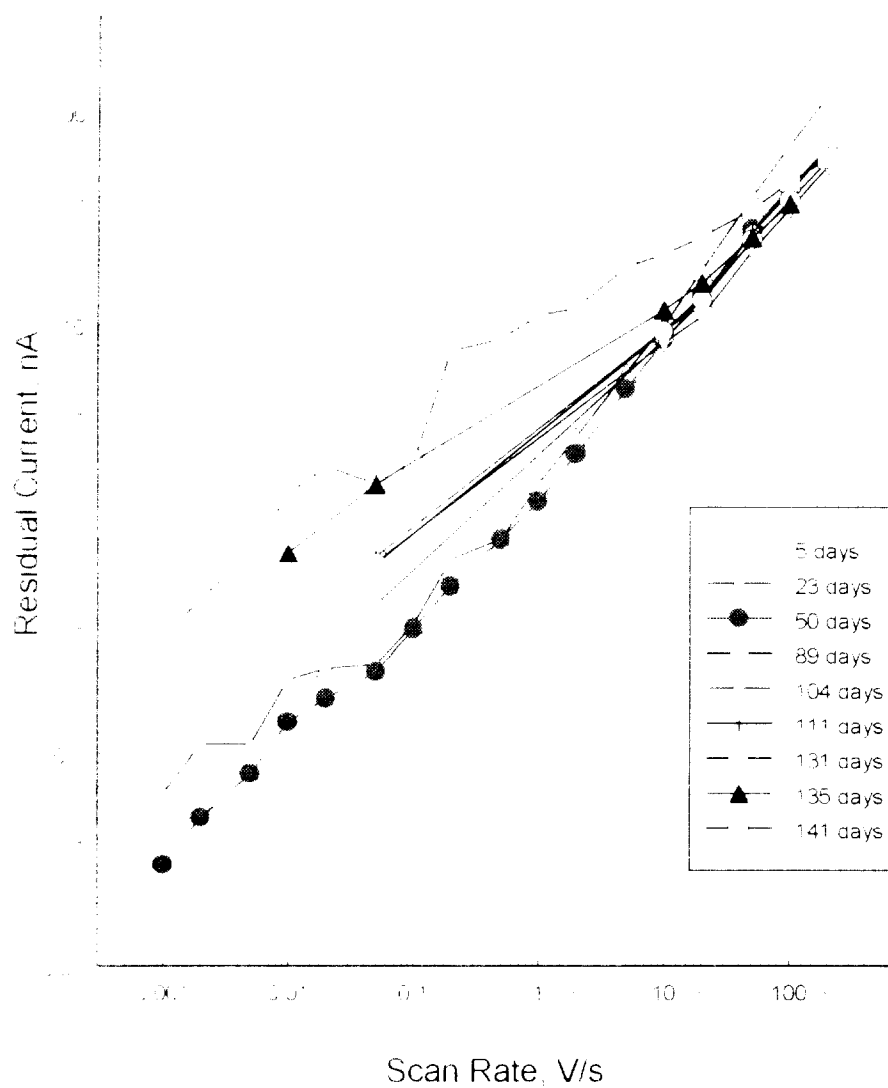


Figure 6 Residual current vs. scan rate for Bak electrode 11B at different times during long term soaking

Iridium Microelectrode 11A
Capp measured in PBS at 0 V vs Ag/AgCl

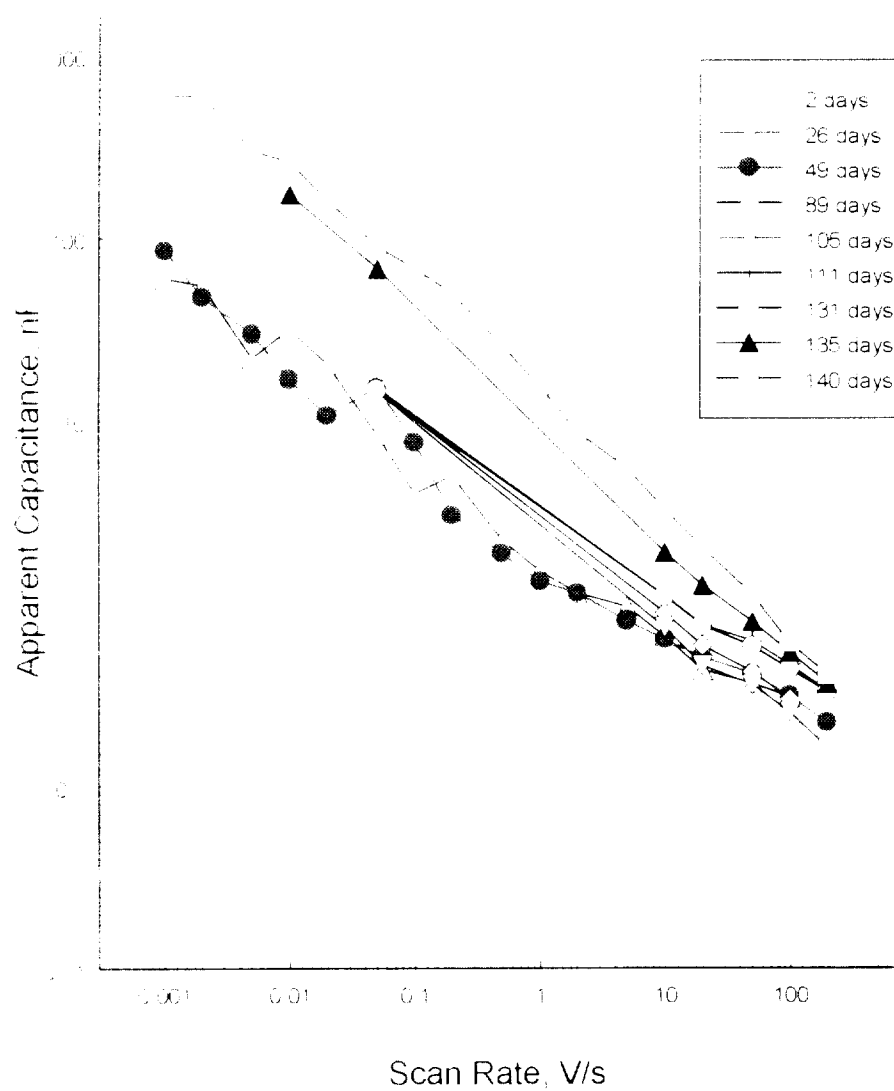


Figure 7 Apparent capacitance vs. scan rate of Bak electrode 11A at different times during long term soaking

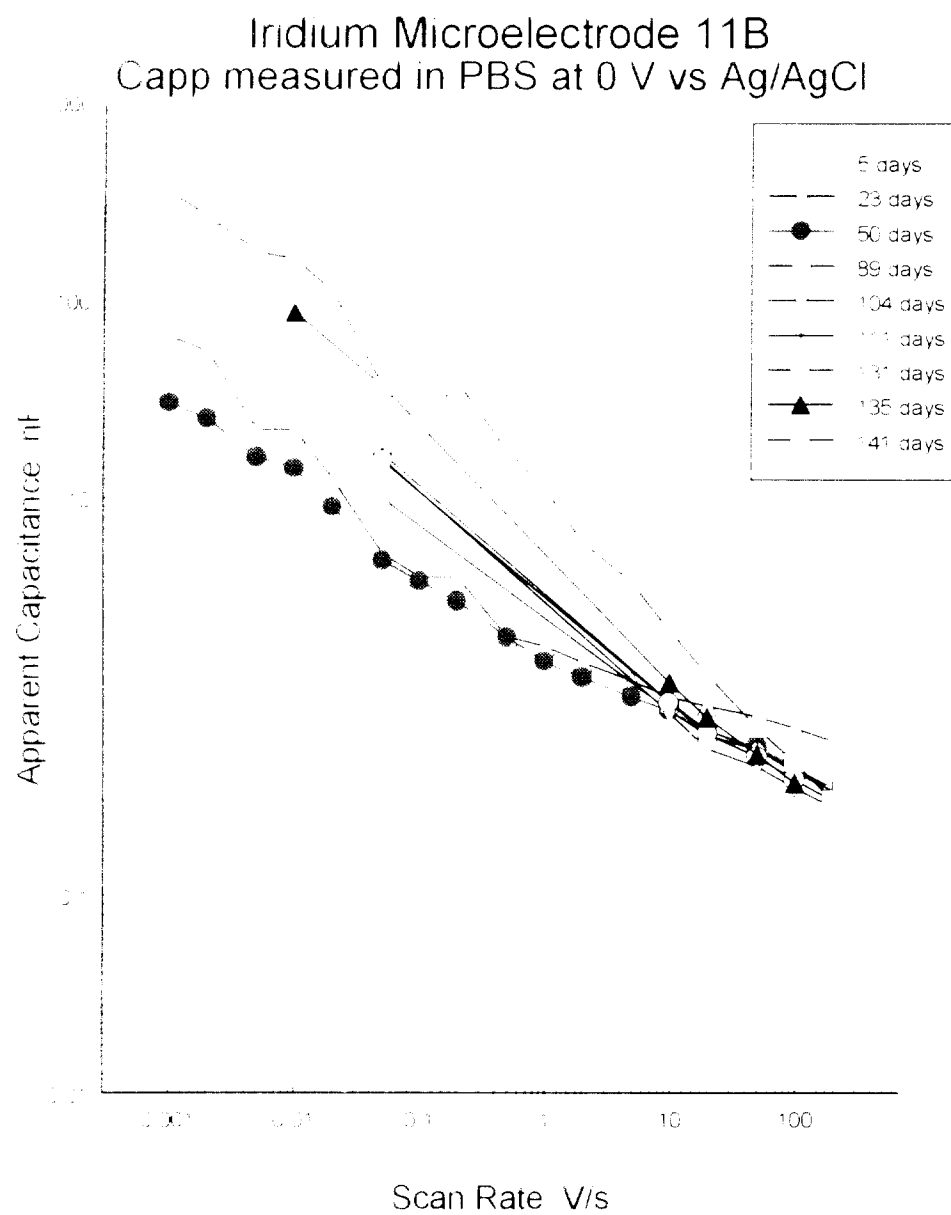


Figure 8 Apparent capacitance vs. scan rate of Bak electrode 11B at different times during long term soaking

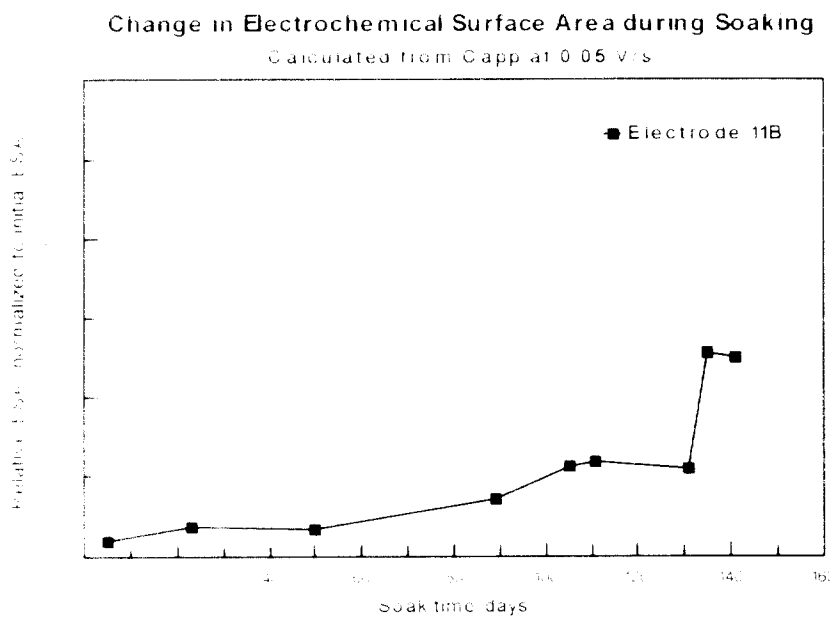
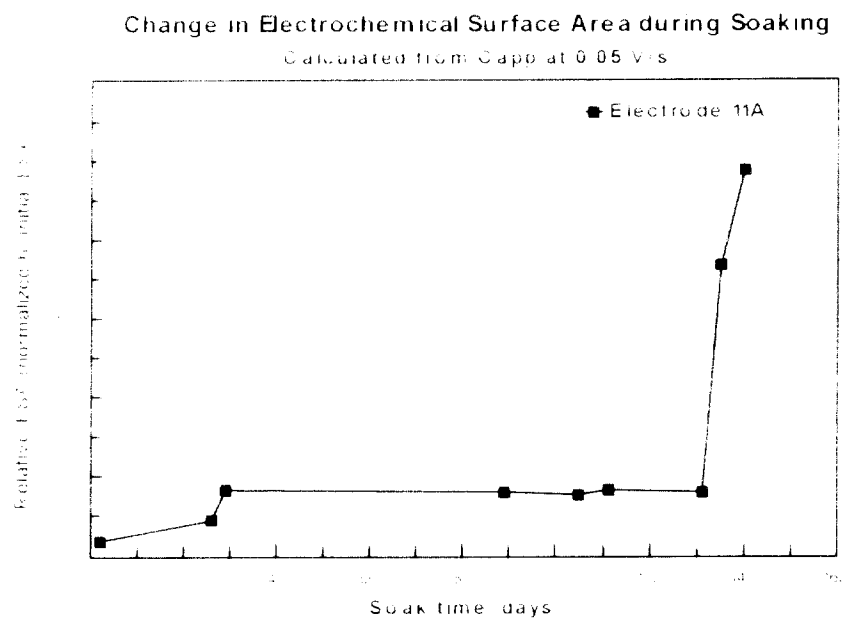


Figure 7. Change in apparent capacitance of Bak electrodes 11A and 11B as measured at 0.05 V/s.

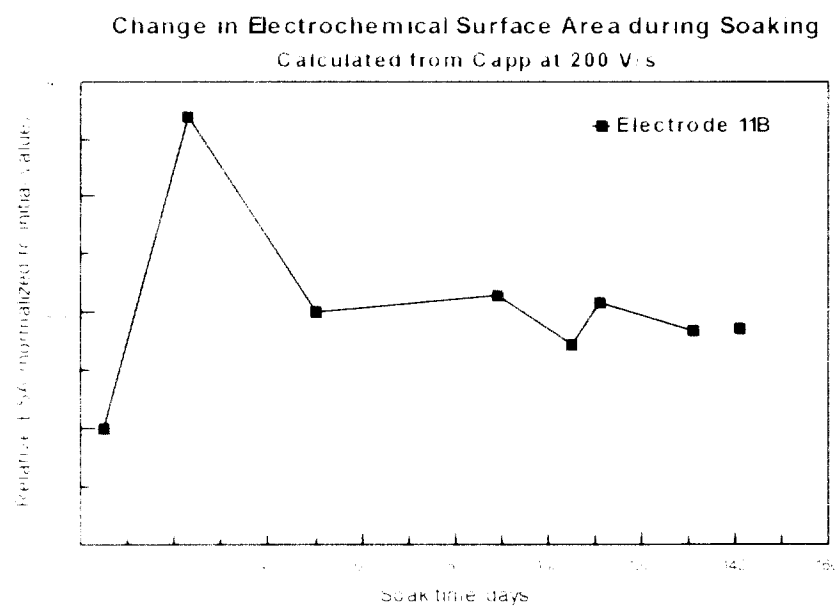
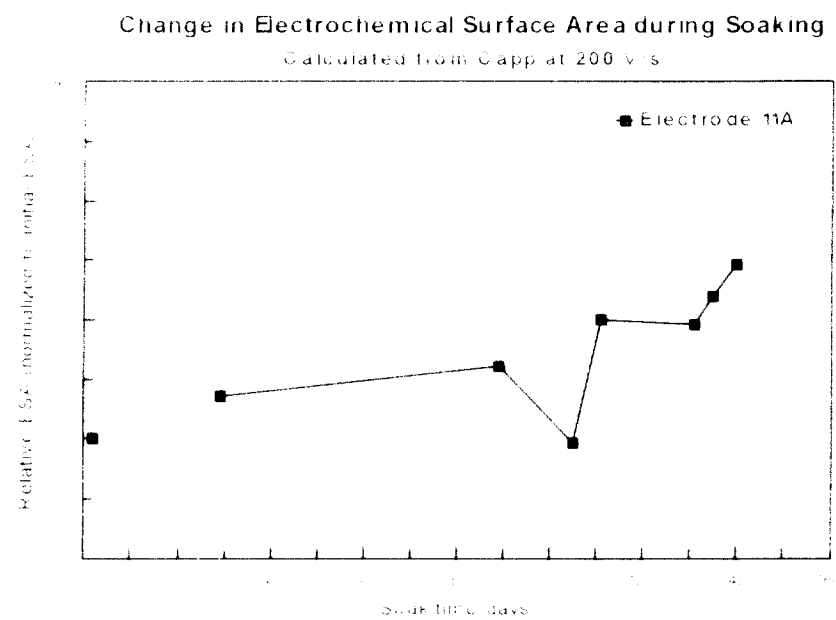


Figure 10 Change in apparent capacitance of Bak electrodes 11A and 11B as measured at 200 V/s

Impedance Spectroscopy Studies

Table 1 lists the impedance at 1 kHz of electrode sites A and B on the dual hatpin assembly at different times during the soaking period. These values are quite erratic and fluctuate by as much as 500-700 k Ω within a period of a few days. Figure 11 shows a plot of the impedance at 1 kHz against soaking time which demonstrates an overall trend toward lower values over the entire soaking period.

Bode representations of the impedance spectra at different times during the soaking period are illustrated in Figure 12. These show a more systematic change in electrode properties. Spectra of both electrodes were quite similar and unremarkable up until day 86 for electrode 11A and day 63 for electrode 11B. However, spectra acquired on day 156 and thereafter displayed a marked change in both magnitude and phase angle. Unfortunately impedance measurements were not made during the intervening period to document the transition in behavior. The decrease in magnitude seen on and after 156 days is associated with a change in phase angle from -80° to -0° , i.e. from capacitive to resistive behavior at frequencies below 100 Hz, and a shift in the time constant to a higher frequency. In addition, the spectra taken on day 156 for electrode 11A show an additional RC element at very low frequencies. This element does not appear in any of the subsequent spectra for that electrode.

The 1 kHz impedance data and particularly the frequency dispersions indicate that significant changes have occurred in both electrodes during the soaking period. The frequency dispersions provide substantially more information than the impedance measurement at a single frequency, but the measurements are not easily obtained, nor are the data easily interpreted. At the present time, it appears that a cyclic voltammetry technique utilizing a range of scan rates and comparison of the residual current at some potential near the open circuit potential of the electrode will be the most useful procedure to adapt for routine *in vivo* use.

Table 2-14 Impedances (k Ω) at 1 kHz of H sites on Mr. Bak electrode No. 11

| Time | Conditions during Impedance Measurement | Site A | Site B |
|------------|----------------------------------------------------------------------------------|--------|--------|
| Before EIC | Measurement by Mr. Bak of initial Z before bubble test | 1550* | 1400* |
| Before EIC | Measurement by Mr. Bak of Z after bubble test | 850* | 800* |
| Day 5 | Initial Impedance in PBS at 100 mV vs Ag/AgCl | 893 | 1,287 |
| Day 6 | Impedance in PBS at OCP, 146 mV | | 585 |
| Day 6 | Impedance in PBS at 100 mV | | 368 |
| Day 7 | Impedance in PBS at OCP, 125 mV | | 374 |
| Day 8 | Impedance in PBS at OCP, 125 mV | | 635 |
| Day 11 | Impedance in PBS at OCP, 130 mV | | 578 |
| Day 12 | Impedance in PBS at OCP, A = -79 mV, B = -124 mV | 831 | 588 |
| Day 13 | Impedance in PBS at OCP, 127 mV | 845 | |
| Day 14 | Impedance in PBS at OCP, 104 mV | 574 | |
| Day 15 | Impedance in PBS at OCP, 49 mV | 570 | |
| Day 18 | Impedance in PBS at OCP, 33 mV | 611 | |
| Day 19 | Impedance in PBS at OCP, 23 mV * | 712 | |
| Day 20 | Impedance in PBS at OCP, A = -21 mV, B = -58 mV * | 1,272 | 403 |
| Day 51 | Impedance in Ru(NH ₃) ₆ Cl ₃ / PBS at 100 mV * | 991 | 1,399 |
| Day 56 | Impedance in PBS at 100 mV | 1,336 | 885 |
| Day 63 | Impedance in PBS at 100 mV | 1,327 | 802 |
| Day 86 | Impedance taken w/out monitor on | 1,277 | |
| Day 156 | Impedance taken at OCP, A = -100 mV, B = -146 mV | 934 | 1,272 |
| Day 185 | Impedance taken at OCP, A = -154 mV, B = -150 | 238 | 541 |
| Day 192 | Impedance taken at OCP, A = -157 mV, B = -100 | 374 | 209 |
| Day 192 | Impedance taken at OCP in new PBS | 430 | 151 |
| Day 201 | Impedance taken at OCP, A = -178, B = -225 | 262 | 564 |
| Day 201 | Impedance taken at OCP in new PBS, A = -171, B = -227 | 276 | 462 |
| Day 208 | Impedance taken at OCP, A = -433, B = -440 | 96 | 216 |

The designation of electrode tips as A or B in Mr. Bak's impedance measurements may not be the same as EIC's identification.

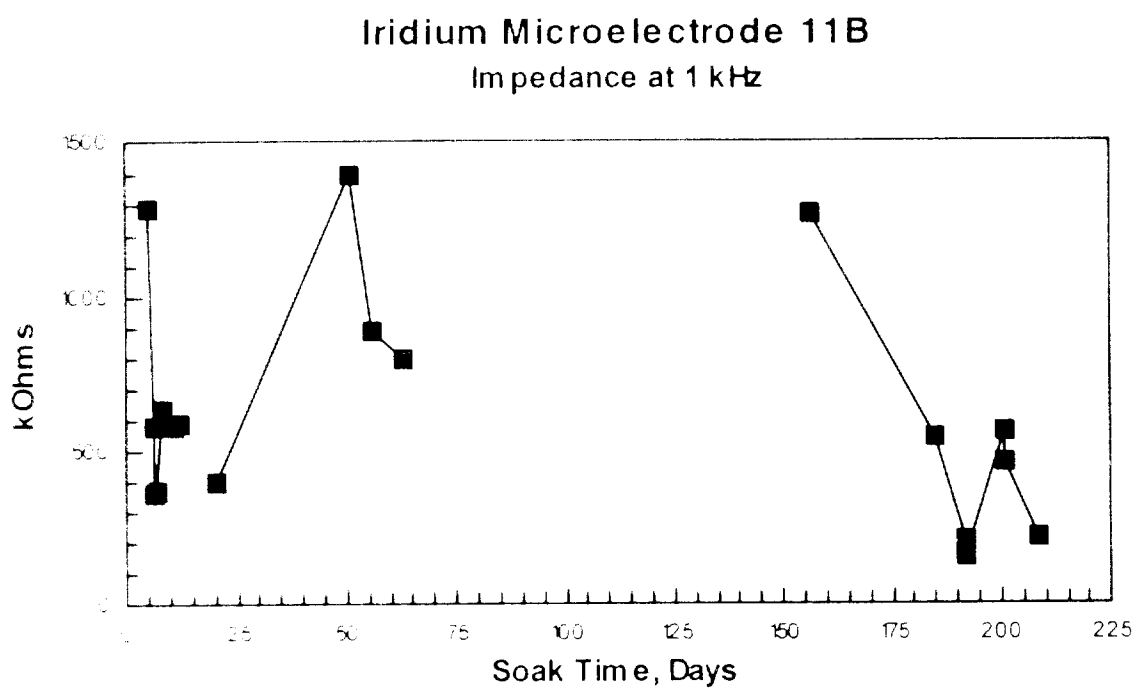
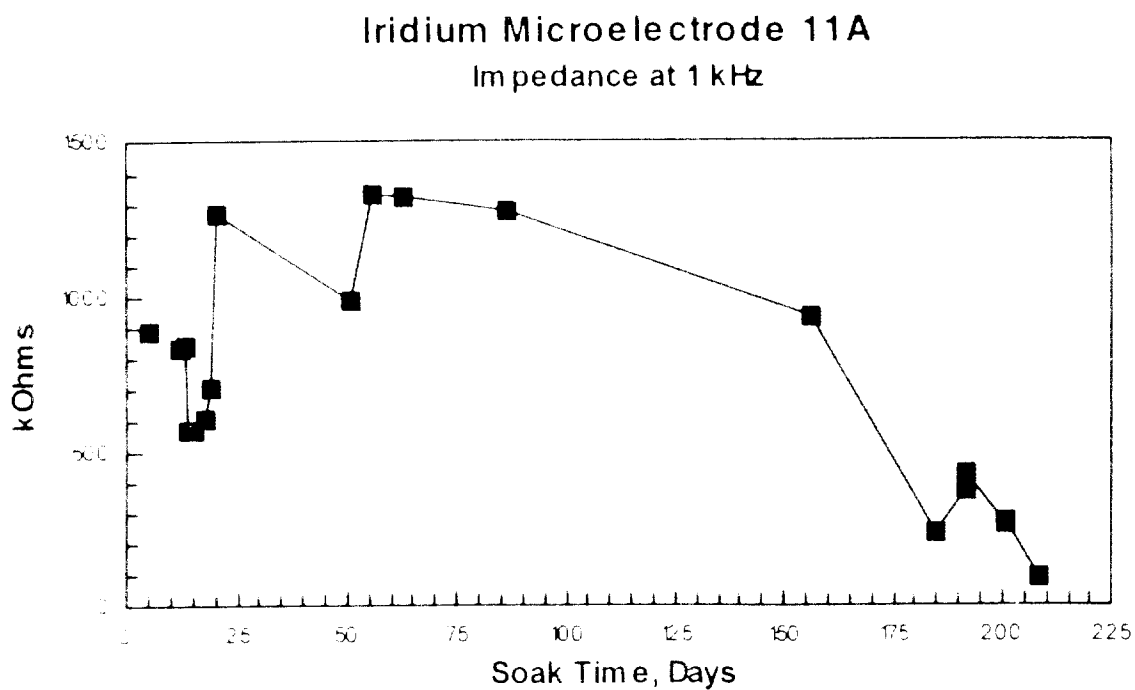
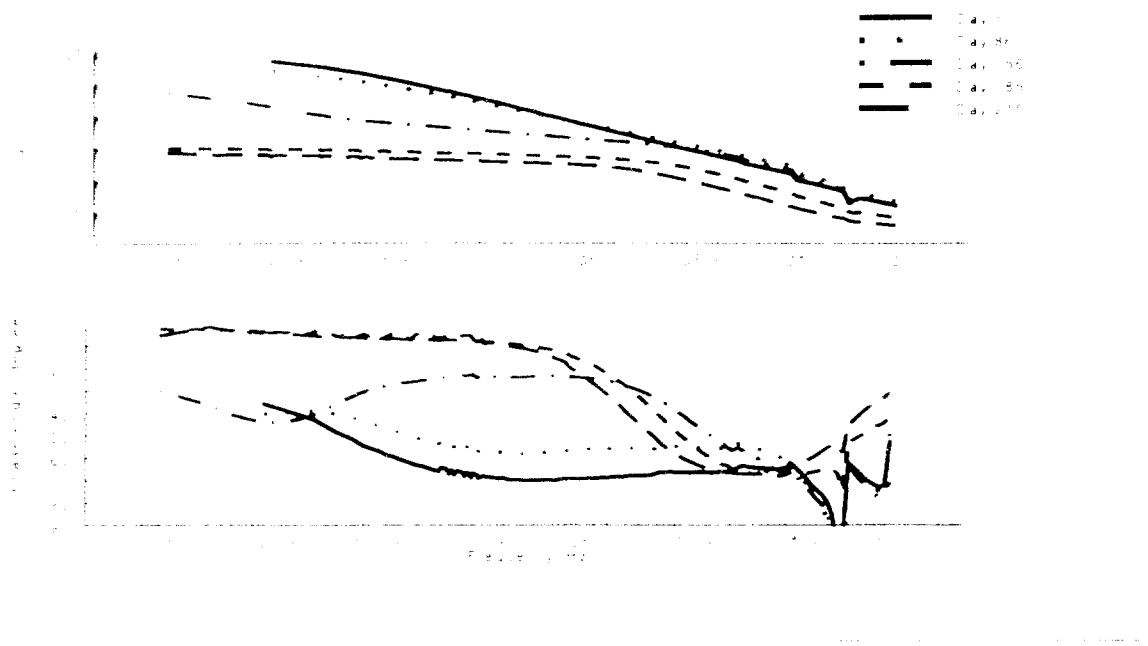


Figure 11 Impedance at 1 kHz of Bak electrodes 11A and 11B at different times during long term soaking

Iridium Microelectrode 11A



Iridium Microelectrode 11B

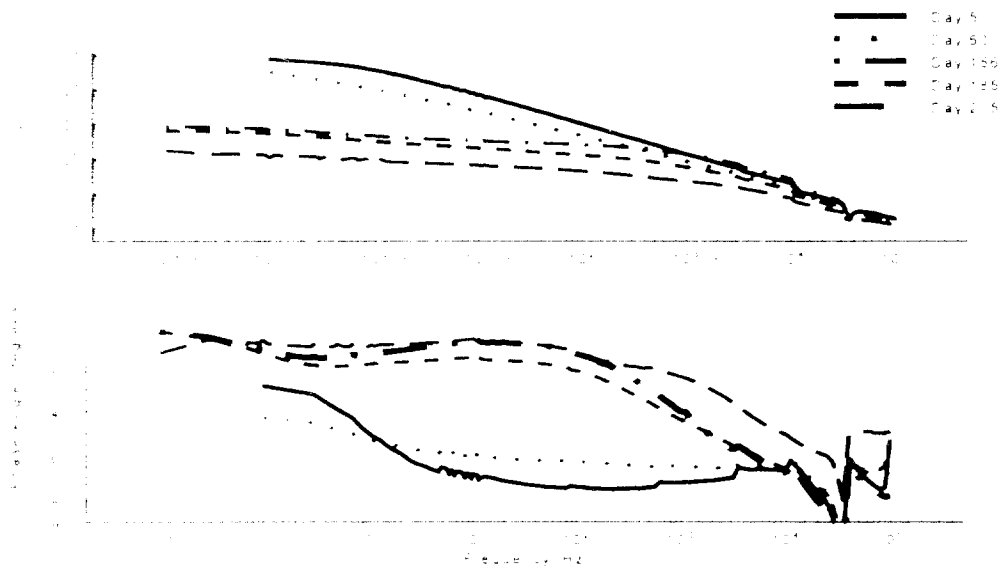


Figure 12 Bode plots of magnitude and phase angle of Bak electrodes 11A and 11B acquired at different times during long term soaking

3.0 WORK FOR NEXT QUARTER

We have received a series of probes with integrated ribbon cables from U-Michigan for use in our electrochemical measurements of Ir microelectrode dimensions and development of a protocol for *in vivo* monitoring of electrochemical stability of Ir microelectrodes. The integrated ribbon cables will permit us to carry out long term soaking studies without any structures other than those fabricated on the wafer being exposed to the electrolyte solution and thereby avoid the previous problems with electrolyte penetration beneath the epoxy encapsulant covering the contact pads. We are now in the process of designing and fabricating a cell assembly with which a ribbon cable probe can be held semi-permanently in the cell with a constant level of immersion into the electrolyte and without danger of damage by inserting and removing the reference electrode and gas bubbler. We have also purchased Ir microelectrodes from World Precision Instruments, Sarasota, FL, having been informed by that company that the electrodes were fabricated by them. We subsequently learned that they were manufactured by MicroProbe whose electrodes we have characterized several times in the past.

4.0 REFERENCES

- Lwardoch, C. M. (1994). Integrity of ultramicrostimulation electrodes determined from electrochemical measurements. J. Applied Electrochem. **24** 835-857.